Magnetic circular dichroism in $L_3M_{2,3}M_{2,3}$ Auger emission from Fe and Co metals due to symmetry-breaking interactions

A. Chassé,[1] H. A. Dürr,[2] G. van der Laan,[3] Yu. Kucherenko,[4] and A. N. Yaresko[4]
[1]*Physics Department, Martin-Luther-University Halle-Wittenberg, D-06099 Halle, Germany*
[2]*BESSY G.m.b.H., D-12489 Berlin, Germany*
[3]*Magnetic Spectroscopy, Daresbury Laboratory, Warrington WA4 4AD, United Kingdom*
[4]*Institute of Metal Physics, National Academy of Sciences of Ukraine, UA-03142 Kiev, Ukraine*
(Received 6 June 2003; published 1 December 2003)

A strong magnetic circular dichroism (MCD) in the $L_3M_{2,3}M_{2,3}$ Auger-electron emission spectra was measured on Fe and Co metal in the off-resonance energy region with the light helicity vector perpendicular to the magnetization direction, despite the fact that this emission is expected to be symmetry forbidden in this geometry. The experimental results are explained quantitatively by taking into account the exchange interaction of the spin-orbit split core states with the spin-polarized valence band. It is shown that the local valence-band magnetic moment is strongly suppressed in the presence of a $2p$ hole in the intermediate state. As a result the MCD signal decreases going from Fe to Co metal, while for Ni the MCD is no longer observable. This behavior is completely different for the measurements at resonance—i.e., at the L_3 absorption edge, where the MCD signal is strong ($\sim 9\%$) for Fe, Co, and Ni due to the large spin polarization of the $2p$ core hole which is caused by unoccupied $3d$ states with predominantly minority spin in the vicinity of the Fermi level.

DOI: 10.1103/PhysRevB.68.214402 PACS number(s): 75.25.+z, 78.20.Ls, 78.70.Dm, 79.60.−i

I. INTRODUCTION

Since the early 1990s the phenomenon of magnetic circular dichroism (MCD)—i.e., the dependence of the spectral intensity on the relative orientation of the magnetization and photon helicity—has been widely used in x-ray spectroscopies for the element-specific analysis of magnetic systems.[1] [MCD is usually understood as the change in absorption when the photon helicity is reversed in a magnetic material. In the case of x-ray absorption spectroscopy (XAS) one could call this ''MCD in XAS,'' although the term x-ray magnetic circular dichroism (XMCD) is also widely accepted. MCD in photoemission can then be understood as the change in photoemission when the photon helicity is reversed. MCD in Auger spectroscopy is the change in the Auger spectra when the photon helicity is reversed. Since this paper specifically deals with Auger spectroscopy, we have in cases where this should not lead to any confusion shortened ''MCD in Auger'' to ''MCD.'' From this nomenclature it is obvious that if the MCD in XAS is zero, it does not follow that the MCD in Auger spectroscopy would be zero.] MCD was observed in x-ray absorption at the K threshold of Fe metal.[2] It has gained huge popularity due to the discovery of the sum rules[3] which can be applied to obtain the ground-state orbital and spin magnetic moments. The $L_{2,3}$ absorption edges of the $3d$ transition-metal systems show large MCD asymmetries [typically $\sim 30\%$ (Ref. 4–7)] that can be used to determine, e.g., the magnetocrystalline anisotropy energy.[8] MCD is also present in x-ray photoemission, where it was observed in the $2p$ core-level spectrum of Fe metal.[9] In the case of photoemission the electron is excited into a continuum state far above threshold that has negligible spin dependence, contrary to the spin-polarized final states just above the Fermi level in the case of x-ray absorption. Consequently, for $2p$ photoemission the MCD effects are often relatively small; however, large MCD signals have been observed in $3p$ core-level photoemission,[10] especially for a chiral geometry.[11–14]

Since MCD in photoemission originates from the combined presence of spin-orbit coupling and exchange splitting in the core level due to the exchange field of the magnetically ordered $3d$ electrons, a quantitative theoretical description can be accomplished in the framework of a relativistic, spin-polarized band theory.[13,15,16] A reliable interpretation of the experimental results is also possible using general photoemission theories[17–19] where the values of the spin-orbit and exchange splitting can be inserted as free parameters which can be either estimated from fully relativistic electronic-structure calculations or obtained by fitting to the experimental spectra.

Dichroic effects have also been observed in Auger-electron emission where the photoexcited core-hole state decays nonradiatively due to Coulomb interaction.[20,21] The Auger process is a coherent second-order process, where the interaction in the two-hole final state (in the case of a core-core-core transition) can give rise to a multiplet structure that displays a different MCD signal for each multiplet component. Auger spectra can be measured either in the on-resonance region (with the photon energy at the core-level excitation threshold—i.e., with x-ray absorption as the excitation step) or off-resonance region (with a primary photoelectron excited into a high-energy continuum state—i.e., with x-ray photoemission as the excitation step). These two excitation conditions result in different intermediate core-hole states, consequently leading to a different MCD.

Only a few papers have been devoted to MCD phenomena in Auger-electron spectra.[22–26] A general theory of electron emission taking into account the second-order autoionization process was given in Ref. 27. This paper also predicted the MCD and spin-polarized spectra at resonance in perpendicular geometry for Ni $L_3M_{2,3}M_{2,3}$, $L_3M_1M_{4,5}$, $L_3M_{2,3}M_{4,5}$, and $L_3M_{4,5}M_{4,5}$. So far, only one theoretical calculation has been performed[26] with the aim to describe

quantitatively the MCD in the experimentally measured Auger spectra of $3d$ metals. In Ref. 26, the MCD in the $L_3M_{2,3}M_{2,3}$ spectrum of ferromagnetic Ni has been calculated using the configuration-interaction model for excitation at the L_3 resonance and the satellite above the edge. The measured Auger spectrum[22] for Ni shows an MCD signal of $\sim 9\%$ in the geometry where the photon helicity vector is perpendicular to the magnetization direction. It should be noted that for this *perpendicular geometry* the MCD in x-ray absorption is forbidden and also the angle-integrated photoemission has no MCD. The observed MCD in Auger is caused by the resonant character of the electron excitation (from the $2p$ core level to the polarized unoccupied $3d$ states). This results in a spin- (and orbital-) polarized core-hole state that decays in the Auger transition.[23] Consequently, one might be expecting that the MCD signal vanishes in the off-resonance region. Indeed, no detectable dichroism could be found in the Ni Auger spectra at higher excitation energies.[22] However, more recently a strong MCD ($\sim 6\%$) in the off-resonant Fe $L_3M_{2,3}M_{2,3}$ Auger has been observed in perpendicular geometry (''symmetry-forbidden'' MCD),[24] which was ascribed to spin-dependent screening of the intermediate core hole state; however, no quantitative description of this phenomenon has been given so far.

The aim of this paper is to study the formation processes of the core-core-core Auger spectra from magnetic materials in more detail and to analyze the factors that contribute to the observed strong MCD, especially in perpendicular geometry. Our theoretical considerations are based on the model that has been successfully applied to describe spin-resolved Auger emission.[28–30] In order to explain quantitatively the observed experimental results, the spin-orbit splitting of core levels and the exchange interaction of the core levels with the polarized valence band (VB) as well as the Coulomb interaction between the two final-state holes have to be taken into account. The calculations of the $L_3M_{2,3}M_{2,3}$ spectra and MCD for ferromagnetic Fe, Co, and Ni have been performed and compared with experimental data. We present MCD measurements for Co metal that provide a ''bridge'' between Fe and Ni metal (the measured MCD of Fe and Ni has been published before[23,24]). A discussion of the experimental and theoretical results for the $3d$ transition-metal series provides an opportunity to look for general trends in observed MCD in relation to the features in the electronic structure of these metals.

This paper is organized as follows. Section II is devoted to the description of the experimental setup and the measurements. The theoretical model is presented and discussed in Sec. III. The details of electronic structure calculations and choice of the model parameters are described in Sec. IV. The results obtained for the Auger spectra and MCD are discussed In Sec. V. Conclusions are drawn in Sec. VI.

II. EXPERIMENTAL PROCEDURE

Measurements were performed at beamline ID12B (currently ID08) of the European Synchrotron Radiation Facility (ESRF) at Grenoble. Circularly polarized radiation with a degree of circular polarization of $85\% \pm 5\%$ of either helicity was generated by a helical undulator. The energy resolution of the beamline was set to 700 meV. Reproducibility of the photon energy was better than 10 meV. Photoelectrons were collected using a hemispherical analyzer with multichannel detection and an acceptance angle of $\pm 20°$ at an emission angle of 60° from the surface normal. This large acceptance angle ensures an averaging over diffraction effects which otherwise would give variations on a scale of a few degrees.

Ultrathin 10 ML (monolayer) Fe films were prepared by evaporation onto a Cu(110) surface under ultrahigh-vacuum conditions at pressures of 1×10^{-10} torr as described in detail in Ref. 31. Co films of 5 ML thickness were deposited onto a Cu(100) surface following Ref. 32. All depositions and subsequent measurements were done at room temperature. C and O contamination was monitored with core-level photoemission and new films were prepared when the contamination level reached more than 10% of a ML. The coverages were calibrated with a quartz microbalance. The films were remanently magnetized using a high-current pulse through a coil near the sample. For both systems the easy direction of magnetization is in the surface plane.[31,32] For all photoemission spectra presented in this work the x-ray incidence direction was perpendicular to the surface. Measurements of the $L_3M_{2,3}M_{2,3}$ resonant photoemission were done at the photon-energy position corresponding to the maximum of the MCD in the Fe and Co L_3 absorption edges. Off-resonance Auger spectra were measured at a photon energy of 900 eV. Prior to taking the photoemission data in perpendicular geometry, it was verified that the MCD in x-ray absorption was completely zero, as it should be.

III. THEORETICAL MODEL

The basic theoretical model used for the description of the Auger process has been briefly described in Refs. 28 and 29 and applied[30] to the Fe $L_3M_{2,3}M_{2,3}$ spectrum in order to interpret the spin-resolved Auger measurements performed at the Fe $2p_{3/2}$ excitation threshold (on-resonance) and at much higher excitation energies (off-resonance). In the current presentation of the general expressions for the calculation of the Auger emission intensities, we put the emphasis on the modifications of the theoretical model that are required to calculate the MCD.

A. Auger emission

We discuss the spectra of the Auger electrons emitted from the crystal with a kinetic energy ε_A and spin σ_A in the direction defined by the vector $\mathbf{k}$. The process is described as the excitation from the ground state of the system (with energy E_g) by photon absorption to an excited intermediate state with energy $E_i = E(c) + \varepsilon_p$, where $E(c)$ is the energy of the system with a core-hole state c and ε_p is the kinetic energy of the photoelectron. The intermediate state decays by an Auger transition to a final state with energy $E_f = E(\beta) + \varepsilon_p + \varepsilon_A$, where $E(\beta)$ is the energy of the system with the two-hole state. The expression for the spin-resolved Auger intensity $I_{\mathbf{u}}$ (where the subscript $\mathbf{u}$ denotes the polarization of the primary photon $\hbar\omega$) can be written in the form

$$I_{\mathbf{u}}(\hbar\omega,\varepsilon_A,\sigma_A,\mathbf{k})=\sum_{\beta}\langle M^2_{\mathbf{u}}(\hbar\omega,\varepsilon_A,\sigma_A,\mathbf{k})\rangle_{\beta}\delta(\hbar\omega+E_g-E_f). \tag{1}$$

We restrict our considerations to the range of ε_A (defined by a set of final states E_f) well separated from the rest of the spectrum, especially from the electrons escaped as a result of a direct photoexcitation, so that there is no interference between photoelectron and Auger-electron waves. This is valid for $L_3M_{2,3}M_{2,3}$ Auger transitions, but not for core-core-valence or core-valence-valence Auger processes in the case of resonant excitation where both direct and indirect channels need to be considered. The Auger transition probabilities $\langle M^2_{\mathbf{u}}\rangle_{\beta}$ can be expressed as[27]

$$\langle M^2_{\mathbf{u}}\rangle_{\beta}=\left|\sum_i \frac{W_{fi}T^{\mathbf{u}}_{ig}}{\hbar\omega+E_g-E_i+i\Gamma_i}\right|^2, \tag{2}$$

where $T^{\mathbf{u}}_{ig}$ and W_{fi} are the matrix elements (ME's) for photoexcitation and Auger decay, respectively, and Γ_i characterizes the lifetime broadening of the intermediate state i. If the energy separation of the intermediate states i is less than $\Gamma_i=\Gamma$, we can integrate Eq. (2) over this energy region and obtain

$$\langle M^2_{\mathbf{u}}\rangle_{\beta}=\frac{\pi}{\Gamma}\left|\sum_i W_{fi}T^{\mathbf{u}}_{ig}\right|^2, \tag{3}$$

which is valid if the photoelectron ε_p has no interaction with the core-hole states and is a pure spectator in the Auger decay. In the presence of core-VB interactions (especially for resonant excitation) Eq. (3) is an approximation that may nevertheless be acceptable if the energy splitting in the core-hole state caused by the interaction with the VB does not exceed the lifetime broadening and cannot be resolved experimentally. In that case the intermediate state of the system can be denoted by quantum numbers that characterize the core hole.

In reality, the removal of the core electron alters the effective potential seen by the remaining electrons which readjust to the new potential. In solids this relaxation process involves also the electrons from the surrounding atoms which will screen the core-hole potential. The exact solution for this time-dependent many-body response is extremely complicated, and several approaches have been suggested to describe these processes theoretically.[33–35] In our simple model the core-hole intermediate state is considered as fully relaxed (cf. Sec. IV), whereas all possible many-body excitations (electron-hole pairs, etc.) accompanying the electron emission process are taken into account by the Doniach-Sunjic profile of the spectral line shape.[36]

Let us now consider the transition ME's given by the shorthand notations $T^{\mathbf{u}}_{ig}$ and W_{fi} in Eqs. (2) and (3). The emitted Auger electron with energy ε_A and spin σ_A is described by a sum over spherical waves characterized by quantum numbers L_A $(=l_A,m_A)$. The amplitude of the outgoing electron wave created by the Auger decay of the core-hole state $|c\rangle$ into the final state $|\beta\rangle$ is given by

$$W_{fi}=\sum_{L_A} B_{L_A\sigma_A}(\mathbf{k})\langle\beta|V|L_A\sigma_A;c\rangle, \tag{4}$$

containing the expectation value of the Coulomb interaction V and the scattering path operator

$$B_{L\sigma}(\mathbf{k})=(-i)^l Y_L(\mathbf{k})+\{\text{scattering contributions}\}, \tag{5}$$

which is widely used to describe photoelectron diffraction.[37–39] The spin dependence of $B_{L\sigma}$ in magnetic samples appears due to the spin-dependent scattering phase shifts δ_l^{σ}. For simplicity, we did not take into account in the present paper the magnetic scattering effects of the outgoing Auger electrons; therefore, only direct-wave contributions were retained for $B_{L\sigma}(\mathbf{k})$ in Eq. (5). The MCD effects caused by the scattering processes will be discussed in our forthcoming work.

The amplitude of the photoelectron wave in the direction $\mathbf{k}_p$ due to absorption of a photon $\hbar\omega$ with polarization $\mathbf{u}$ (i.e., the probability amplitude for creation of the core-hole state $|c\rangle$) can be written as

$$T^{\mathbf{u}}_{ig}=\sum_{L_p} B_{L_p\sigma_p}(\mathbf{k}_p)\langle c|\mathbf{u}\cdot\mathbf{r}|L_p\sigma_p\rangle. \tag{6}$$

In Auger spectroscopy (in contrast to Auger-photoelectron coincidence spectroscopy[40,41]) only the emitted Auger electrons are measured. Therefore, the final expressions for the electron emission intensity should be averaged over all photoelectron final states. The energy of the photoelectron ε_p is defined by the energy of the incident photon and it will be important to evaluate the radial part in the dipole ME; cf. Eq. (16). After integration over all directions $\mathbf{k}_p$ the interference of different photoelectron waves does not contribute to the Auger-electron intensity [due to the orthogonality of the $Y_{l_pm_p}(\mathbf{k}_p)$ functions] and we only need to sum the intensity terms over L_p and σ_p.

Using the basis vectors[42]

$$\mathbf{e}_{-1}=\frac{1}{\sqrt{2}}(\mathbf{e}_x-i\mathbf{e}_y),\quad \mathbf{e}_0=\mathbf{e}_z,\quad \mathbf{e}_{+1}=-\frac{1}{\sqrt{2}}(\mathbf{e}_x+i\mathbf{e}_y), \tag{7}$$

we can write the photon polarization in terms of its spherical components

$$\mathbf{u}=u^{-1}\mathbf{e}_{-1}+u^0\mathbf{e}_0+u^{+1}\mathbf{e}_{+1}. \tag{8}$$

The angular part of the dipole operator can be expressed in spherical harmonics as[43]

$$\mathbf{u}\cdot\mathbf{e}=\sqrt{\frac{4\pi}{3}}\left[u^{-1}Y_{1-1}(\mathbf{e})+u^0Y_{10}(\mathbf{e})+u^{+1}Y_{1+1}(\mathbf{e})\right], \tag{9}$$

and the dipole ME reads

$$\langle c|\mathbf{u}\cdot\mathbf{r}|L_p\sigma_p\rangle=\sum_q u^q\langle c|rY_{1q}(\mathbf{e})|L_p\sigma_p\rangle, \tag{10}$$

with $q=-1,\ 0,+1$ and $\mathbf{e}=\mathbf{r}/r$. Finally, Eq. (3) can be brought into the form

$$\langle M_{\mathbf{u}}^2\rangle_\beta=\sum_{L_p\sigma_p}|u^{-1}F_{-1}+u^0F_0+u^{+1}F_{+1}|^2, \tag{11}$$

where the amplitudes F_q correspond to the components of the polarization vector, which can be written as

$$F_q=\frac{\pi}{\Gamma}\sum_c\sum_{L_A}B_{L_A\sigma_A}(\mathbf{k})\langle\beta|V|L_A\sigma_A;c\rangle\langle c|rY_{1q}(\mathbf{e})|L_p\sigma_p\rangle. \tag{12}$$

In the case of the four one-electron states $|lm\sigma\rangle$ we have

$$\langle ij|V|Ac\rangle=\sum_{\lambda\mu}(-1)^\mu\mathcal{R}_\lambda(ci;jA)\times\sqrt{\frac{(2l_i+1)(2l_j+1)}{(2l_c+1)(2l_A+1)}}\times C^{l_cm_c}_{l_im_i,\lambda-\mu}C^{l_c0}_{l_i0,\lambda0}C^{l_Am_A}_{l_jm_j,\lambda\mu}C^{l_A0}_{l_j0,\lambda0}\delta_{\sigma_c\sigma_i}\delta_{\sigma_A\sigma_j}, \tag{13}$$

where the radial integrals take the form

$$\mathcal{R}_\lambda(ci;jA)=2e^{i\delta^{\sigma_A}_{l_A}}\int r_1^2dr_1\int r_2^2dr_2\times R_{l_A}(\varepsilon_A,r_1)R_{l_c}(r_2)\frac{r_<^\lambda}{r_>^{\lambda+1}}R_{l_i}(r_2)R_{l_j}(r_1), \tag{14}$$

and the products of Clebsch-Gordan coefficients[42] $C^{lm}_{l_im_i,l_jm_j}$ arise from integrations over the angular part of the ME. The dipole ME describing the excitation of the core state $|l_cm_c\sigma_c\rangle$ due to absorption of a photon with polarization vector $\mathbf{u}=\mathbf{e}_q$ has the form

$$\langle c|rY_{1q}(\mathbf{e})|L_p\sigma_p\rangle=\mathcal{R}(c;p)\sqrt{\frac{2l_c+1}{2l_p+1}}C^{l_pm_p}_{l_cm_c,1q}C^{l_p0}_{l_c0,10}\delta_{\sigma_c\sigma_p}, \tag{15}$$

with radial part

$$\mathcal{R}(c;p)=e^{i\delta^{\sigma_p}_{l_p}}\int r^3drR_{l_p}(\varepsilon_p,r)R_{l_c}(r). \tag{16}$$

The actual wave functions used in the calculations can be expressed as linear combinations of the $|lm\sigma\rangle$ functions (cf. Sec. III B) and, consequently, the actual ME's are expressed in terms of Eqs. (13) and (15) according to the required representations of the wave functions.

B. Spin-orbit and exchange interaction

In order to calculate the dipole and Auger transition ME's we first determine the one-particle wave functions $|\psi_\nu\rangle$ that include both spin-orbit and exchange interaction due to an effective spin field. These contributions to the one-particle Hamiltonian are given by

$$H_{\text{int}}=\lambda\mathbf{l}\cdot\mathbf{s}+\xi s_z, \tag{17}$$

with a spin-orbit splitting $\Delta_{\text{so}}=(2l+1)\lambda/2$ and an exchange splitting $\Delta_{\text{ex}}=\xi$. This approach is similar to that applied in Refs. 16,18,19, and 44 to the photoemission process and was recently used in Ref. 30 to describe spin-resolved Auger spectra. A reasonable choice for the eigenfunctions is the spin-orbit part of the Hamiltonian with basis functions

$$|jl\mu\rangle=\sum_{m\sigma}C^{j\mu}_{lm,\frac{1}{2}\sigma}|lm\sigma\rangle. \tag{18}$$

For the $2p$ and $3p$ core levels the exchange interaction leads to a mixing of the $j=\frac{3}{2}$ and $\frac{1}{2}$ states that have the same value of μ (which is still a good quantum number):

$$|\psi_\nu(\mu)\rangle=c^{(+)}_{\nu\mu}(\xi)\left|\frac{3}{2},1,\mu\right\rangle+c^{(-)}_{\nu\mu}(\xi)\left|\frac{1}{2},1,\mu\right\rangle. \tag{19}$$

By substituting Eq. (18) into (19) the functions $|\psi_\nu\rangle$ can be expressed in terms of $|lm\sigma\rangle$; however, the coefficients of this linear combination,

$$A^{m\sigma}_\nu=c^{(+)}_{\nu\mu}(\xi)C^{\frac{3}{2}\mu}_{lm,\frac{1}{2}\sigma}+c^{(-)}_{\nu\mu}(\xi)C^{\frac{1}{2}\mu}_{lm,\frac{1}{2}\sigma} \tag{20}$$

have lost the symmetry properties of the Clebsch-Gordan coefficients, in particular $\{m,\sigma\}\rightarrow\{-m,-\sigma\}$.

The two-hole final state $|\beta\rangle$ can be expressed by a Slater determinant, so that the Auger ME contains the Coulomb integral and the corresponding exchange integral that differs from Eqs. (13) and (14) by an interchange $i\leftrightarrow j$. Further, the correlated two-hole final state $|\beta\rangle$ displays a multiplet structure with the individual LS terms separated in energy. The two-particle states can be described by $|LS;JM_J\rangle$ functions constructed by angular momentum summation and transformation relations[42,45,46] as

$$|j_1j_2;JM_J\rangle=\sum_{\mu_1\mu_2}C^{JM_J}_{j_1\mu_1,j_2\mu_2}|j_1l_1\mu_1\rangle|j_2l_2\mu_2\rangle, \tag{21}$$

$$|LS;JM_J\rangle=\sum_{j_1j_2}\zeta\begin{Bmatrix}l_1&\frac{1}{2}&j_1\\ l_2&\frac{1}{2}&j_2\\ L&S&J\end{Bmatrix}|j_1j_2;JM_J\rangle,$$

$$\zeta=[(2L+1)(2S+1)(2j_1+1)(2j_2+1)]^{1/2}. \tag{22}$$

The $L_3M_{2,3}M_{2,3}$ process leads to a $3p^4$ configuration (two final-state holes in the $3p$ shell) with three LS components: two singlet states($^1S,{}^1D$) and one triplet state (^3P). Their energies are given in LS coupling by the relations

$$E(^1S)=F^{(0)}+10F^{(2)},$$

$$E(^1D)=F^{(0)}+F^{(2)},$$

$$E(^3P)=F^{(0)}-5F^{(2)}, \tag{23}$$

where the values of $F^{(0)}$ and $F^{(2)}$ relate to the Coulomb integrals for the $3p$ core shell.[46]

After the spin-orbit interaction and the exchange interaction with the VB electrons, Eq. (17), are included for both electrons, the two-particle Hamiltonian is diagonalized. Details of this procedure will be described elsewhere.[46,47] The most important result are the eigenfunctions expressed as linear combinations of pure $|LS;JM_J\rangle$ states. The spin-orbit interaction leads to a mixing of the states with the same J, M_J values; namely, the $^1S_0$ component is coupled with the $^3P_0$, while the $^1D_2$ components are coupled with the corresponding M_J components of the $^3P_2$. The exchange interaction couples the components with the same L, S, M_J values, but different J, so that the corresponding M_J components of all ^3P_J states are mixed. Consequently, including both spin-orbit and exchange interaction couples *all* $|LS;JM_J\rangle$ states and will result in redistribution of the spectral weight.

C. Magnetic circular dichroism

First, we define the coordinate system with respect to the surface normal direction (chosen as the x axis), so that the sample surface coincides with the yz plane. The magnetization vector is parallel to the quantization axis z. The direction of the incoming photon is considered to be in the xz plane and defined by the angle θ with respect to z. Then, the polarization vector for right (left) circularly polarized photons is given as

$$\mathbf{u}_{R(L)}=\frac{\sqrt{2}}{2}(\cos\theta\mathbf{e}_x\mp i\mathbf{e}_y+\sin\theta\mathbf{e}_z) \tag{24}$$

or, in the spherical basis of Eq. (7),

$$\mathbf{u}_R=\frac{1}{2}(1+\cos\theta)\mathbf{e}_{-1}+\frac{\sqrt{2}}{2}\sin\theta\mathbf{e}_0+\frac{1}{2}(1-\cos\theta)\mathbf{e}_{+1},$$

$$\mathbf{u}_L=-\frac{1}{2}(1-\cos\theta)\mathbf{e}_{-1}+\frac{\sqrt{2}}{2}\sin\theta\mathbf{e}_0-\frac{1}{2}(1+\cos\theta)\mathbf{e}_{+1}. \tag{25}$$

Substitution of the coordinates of the polarization vector into Eq. (11) and taking the difference in the emission intensities for right- and left-circularly polarized photons yields

$$\begin{aligned}\Delta I_\beta(\mathbf{k})&=\langle M_R^2\rangle_\beta-\langle M_L^2\rangle_\beta\\&=\sum_{L_p\sigma_p}\Big[(|F_{-1}|^2-|F_{+1}|^2)\cos\theta+(F_{-1}^*F_0+F_{+1}^*F_0\\&\quad+F_{-1}F_0^*+F_{+1}F_0^*)\frac{\sqrt{2}}{2}\sin\theta\Big].\end{aligned} \tag{26}$$

Thus, when the photon direction is parallel or antiparallel to the magnetization vector ($\theta=0°$ or 180°) the MCD signal is determined only by the diagonal terms $|F_q|^2$, while in perpendicular geometry ($\theta=90°$) the MCD signal appears due to interference of the waves F_q whereas the diagonal terms vanish.[26]

In the following we will restrict our considerations to the perpendicular geometry and study the $\mathbf{k}$ dependence (i.e., the Auger-electron emission direction) of the MCD effect. First, we assume that the radial parts of ME's are independent of the spin and that the polarized VB states do not influence the excitation and emission processes.

Taking into account the transformation of a spinor with respect to the reflection and rotation operations,[48] we find the following symmetry properties for the Auger emission intensity $I_{\mathbf{u}}(\sigma_A,\mathbf{k})$ in Eq. (1) (the direction $\mathbf{k}$ is defined by polar angles ϑ,φ with respect to z).

(i) For reflection through the xy plane,

$$I_{\mathbf{u}}(\sigma_A,\vartheta,\varphi)=I_{\mathbf{u}^*}(\sigma_A,\pi-\vartheta,\varphi); \tag{27}$$

(ii) for 180° rotation around the x axis,

$$I_{\mathbf{u}}(\sigma_A,\vartheta,\varphi)=I_{\mathbf{u}}(-\sigma_A,\pi-\vartheta,-\varphi), \tag{28}$$

where the subscript $\mathbf{u}^*$ denotes the reversal of the photon helicity from right to left circular polarization or vice versa.

After Eqs. (27) and (28) have been applied to Eq. (11), we can deduce the symmetry properties of the amplitudes F_q. Taking advantage of the symmetry properties of Clebsch-Gordan coefficients[42] in the angular parts of the ME's, Eqs. (13) and (15) as well as Eq. (18), we have for arbitrary $\mathbf{k}$ direction

$$\begin{aligned}F_0(l_p,m_p,\sigma_p,\sigma_A)&=\tau F_0(l_p,-m_p,-\sigma_p,-\sigma_A),\\F_{\pm1}(l_p,m_p,\sigma_p,\sigma_A)&=-\tau F_{\mp1}(l_p,-m_p,-\sigma_p,-\sigma_A),\end{aligned} \tag{29}$$

with $\tau=1$ and -1 for triplet and singlet two-hole final states, respectively. These symmetry relations are similar to those for photoelectron emission which can be deduced from the general expressions presented in Ref. 43. In the case of Auger emission the spin symmetry of the two-hole final state [the interchange $i\leftrightarrow j$ in Eq. (13)] should be in addition taken into account. Performing the summation over L_p,σ_p in Eq. (26) and then summing the emission intensities over σ_A, one can see that all terms cancel each other due to the symmetry in Eq. (29). Thus in perpendicular geometry there is no MCD in spin-integrated Auger-electron emission for all emission directions.

In order to observe an MCD signal in perpendicular geometry, the symmetry conditions have to be broken. Equation (29) is no longer valid if we take into account that the values of the radial ME's vary slightly for different spin states. However, as shown by the calculations below, the influence on the MCD signal due to the spin dependence in the radial ME's is very small.

The individual contributions to the MCD signal do not cancel in the spin-resolved Auger-electron detection [the symmetry of Eq. (29) is broken due to a preferred σ_A value], in which case MCD might be present. It should also be noted that the spin polarization of the emitted Auger wave reverses sign when the emission direction traverses the xy plane. For a particular partial wave l_A the spin polarization must vanish in the xy plane, whereas for the total intensity the plane of zero polarization is rotated around the x axis due to the interference of the partial Auger waves [cf. the sum over L_A in the amplitude of Eq. (12)] and does not coincide with the xy

plane. The direction of this rotation is opposite for right- and left-circularly polarized photons. For normal emission (along x) the Auger-electron intensity is not spin polarized.

The symmetry in Eq. (29) is also broken in the case of additional restricting requirements to the photoelectron spin states σ_p. If the photoelectron is excited into a spin-polarized state, as realized at resonance in magnetic $3d$ metals, the amplitudes for σ_p and $-\sigma_p$ are different and, consequently, a strong MCD signal can be observed.

Now let us take into account the exchange interaction of core states with the spin-polarized VB states. As discussed in Sec. III B, this leads to a modification of amplitudes caused by the mixing of the $p_{3/2}$ and $p_{1/2}$ states. In more detail, using Eqs. (19) and (20) we obtain for the mixed states derived from the $|\frac{3}{2},1,\pm\frac{1}{2}\rangle$ functions

$$\left|\psi_{3/2}\left(-\frac{1}{2}\right)\right\rangle = \left[c^{(+)}_{3/2,-1/2}(\xi)\sqrt{\frac{1}{3}} - c^{(-)}_{3/2,-1/2}(\xi)\sqrt{\frac{2}{3}}\right] Y_{1-1}\chi_+ + \left[c^{(+)}_{3/2,-1/2}(\xi)\sqrt{\frac{2}{3}} + c^{(-)}_{3/2,-1/2}(\xi)\sqrt{\frac{1}{3}}\right] Y_{10}\chi_-,$$

$$\left|\psi_{3/2}\left(+\frac{1}{2}\right)\right\rangle = \left[c^{(+)}_{3/2,+1/2}(\xi)\sqrt{\frac{2}{3}} - c^{(-)}_{3/2,+1/2}(\xi)\sqrt{\frac{1}{3}}\right] Y_{10}\chi_+ + \left[c^{(+)}_{3/2,+1/2}(\xi)\sqrt{\frac{1}{3}} + c^{(-)}_{3/2,+1/2}(\xi)\sqrt{\frac{2}{3}}\right] Y_{11}\chi_-, \quad (30)$$

and the transformation $\{m,\sigma\}\rightarrow\{-m,-\sigma\}$ can be compensated by changing $\mu\rightarrow-\mu$ only for $c^{(+)}_{\nu\mu}=1$ and $c^{(-)}_{\nu\mu}=0$—i.e., for the pure $|jl\mu\rangle$ without exchange mixing. Otherwise, the symmetry in the emission intensities with respect to the spin inversion is broken, and, e.g., Eq. (28) is not valid.

Due to the amplitude redistribution by the exchange mixing in the $2p$ sublevels, the MCD signal in the $L_3M_{2,3}M_{2,3}$ spectrum must be (formally) compensated by an MCD signal of opposite sign in the $L_2M_{2,3}M_{2,3}$ spectrum. The exchange mixing between the $3p$ sublevels cannot lead to an MCD in the integral intensities (calculated as a sum over all possible two-hole final states) but causes changes in the weights of the individual multiplet components that depend on the photon helicity. As a result, the different multiplet components will have MCD signals with different signs, which should cancel in the MCD spectrum integrated over the whole spectrum.

Note that when the exchange interaction is included, the symmetry relation of Eq. (27) still holds and, consequently, for Auger emission directions **k** in the xy plane ($\vartheta=90°$) there is no MCD. Thus in perpendicular geometry for all cases (on- and off-resonance excitation, spin-resolved and spin-integrated detection of Auger electrons) the MCD is symmetry forbidden only for emission directions **k** that are perpendicular to the magnetization direction.

IV. ELECTRONIC STRUCTURE OF THE MAGNETIC 3*d* TRANSITION METALS

A. Energy-band structure and local magnetic moments

The energy-band structure of ferromagnetic bcc Fe, hcp Co, and fcc Ni metal was calculated using the self-consistent linear muffin-tin orbitals (LMTO) method in the atomic-sphere approximation.[49,50] The calculations were performed within the scalar-relativistic formalism for the VB states whereas fully relativistic solutions were used for the core levels. The exchange and correlation effects were taken into account using the local-density approximation (LDA) with the parametrization for the exchange-correlation potential given in Ref. 51.

In the theoretical model described in Sec. III it is assumed that in the intermediate state the system is fully relaxed. In order to estimate the actual parameter values of the Auger decay we have also performed calculations for an atom with a $2p$ core hole embedded in the crystal (in the following this atom is called the emitter). These self-consistent calculations for a $2p$ hole screened by VB electrons were performed within a supercell approach. A supercell containing 16, 24, and 32 atoms was chosen for Fe, Co, and Ni, respectively, ensuring a good convergence of the local electronic structure at the emitter.

The calculated density of states (DOS) for the majority and minority spins is shown in Fig. 1. The partial occupation numbers as well as the local magnetic moments are listed in Table I. The screening process leads to an increase in the local valence charge and to a redistribution of the VB DOS. In the considered $3d$ metals the core-hole screening has d character. Moreover, the screening process leads to a reduction in the number of s and p electrons in Fe and Co, whereas in Ni this number slightly increases. It should also be noted that in Fe and Co the increased number of valence electrons leads even to a negative charging (~ 0.08) of the atomic sphere of the emitter at the cost of the surrounding atoms. The screening electrons occupy mainly the minority-spin $3d$ states and the local magnetic moment of the emitter site is strongly reduced. It is interesting to note that the local magnetic moment of the emitter is very close to that of a ground-state atom with incremented atomic number (as predicted by a simple $Z+1$ approximation). Thus the screened emitter in Ni has a negligibly small magnetic moment, like in Cu. However, a similar statement cannot be made for the DOS.

Another important property required for the MCD calculations is the spin polarization of the unoccupied $3d$ states above the Fermi level E_F (which are the final states that will be occupied by the excited electron in the case of on-resonant excitation). It is not appropriate to use the values defined by the DOS directly at E_F (e.g., for Fe the majority-spin states are still dominant at E_F; see Table I). Taking into account the energy distribution of the incident photons as well as various energy broadenings due to the excitation processes, we have chosen an energy region covering 1 eV above E_F that accepts the electrons excited at the L_3 thresh-

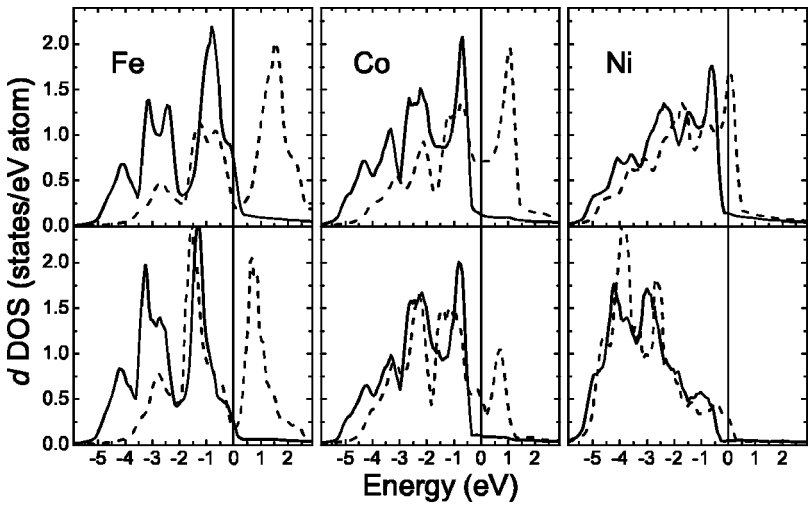

FIG. 1. Calculated majority-spin (solid lines) and minority-spin (dashed lines) $3d$ DOS for Fe, Co, and Ni metal in the ground state (upper panels) and in the presence of a $2p$ core hole (lower panels).

old. The minority-to-majority ratio of the unoccupied $3d$ states in this energy range is 2.34, 9.63, and 5.74 for Fe, Co, and Ni, respectively. Note that while Ni has the highest minority-spin DOS at E_F, Co has the maximum minority-to-majority ratio as estimated from the integrated DOS.

B. Parameters of the calculation

The main parameters in the theoretical model are the spin-orbit parameter λ and the exchange parameter ξ, which define the mixing of the $|jl\mu\rangle$ states and, in the final analysis, the value of the MCD signal. Their values were estimated from the calculated energy splitting in the $2p$ and $3p$ levels in atoms with the given local magnetic moments (see Table II). In comparison to the ground state, the spin-orbit splitting is slightly increased in the presence of a $2p$ hole due to localization of the wave functions in the core-hole potential, whereas the exchange splitting decreases due to a strongly reduced local magnetic moment.

The calculated values of λ and ξ for ground-state atoms in Fe and Ni agree well with those calculated in Ref. 16. However, the calculated value for ξ_{3p} appears to be rather high. In order to reproduce the MCD and spin polarization in the experimental photoemission spectra of Fe, the authors of Ref. 16 used scaled values of $\lambda=0.87$ eV and $\xi=1.17$ eV for the $3p$ level instead of the calculated $\lambda=1.04$ eV and $\xi=2.44$ eV. The corresponding parameters for Ni were also scaled by a factor of 0.95 and 0.37, respectively. The data for the spin-orbit and exchange splittings[18,44,52,53] extracted from the experimental core-level photoemission spectra of Fe support the statement that in the ground state of Fe atoms the ξ/λ ratio for the $3p$ level is between 1.0 and 1.3 (despite the

TABLE I. Calculated density of unoccupied $3d$ states at E_F and between E_F and $(E_F+1.0$ eV), the VB occupation for *s*, *p*, and *d* states, and the local spin moments (total values and those produced by $3d$ electrons).

	Fe		Co		Ni	
	Majority spin	Minority spin	Majority spin	Minority spin	Majority spin	Minority spin
Ground state						
$3d$ DOS at E_F (in $\frac{\text{states}}{\text{eV atom}}$)	0.903	0.201	0.122	0.696	0.142	1.509
$3d$ DOS integrated from E_F to $(E_F+1.0$ eV) (in $\frac{\text{states}}{\text{atom}}$)	0.173	0.405	0.100	0.960	0.107	0.614
VB occupation						
n_s	0.314	0.328	0.318	0.333	0.325	0.330
n_p	0.358	0.417	0.351	0.415	0.364	0.390
n_d	4.462	2.120	4.621	2.962	4.608	3.983
M_{total} (M_d) (in μ_B)	2.270(2.342)		1.580 (1.659)		0.595 (0.625)	
Excited state ($2p$ *hole)*						
VB occupation						
n_s	0.304	0.325	0.306	0.327	0.326	0.334
n_p	0.347	0.417	0.340	0.410	0.371	0.399
n_d	4.714	2.980	4.694	4.007	4.797	4.763
M_{total} (M_d) (in μ_B)	1.643(1.734)		0.595 (0.687)		-0.002 (0.035)	

TABLE II. Calculated spin-orbit and exchange splitting (in eV) for the $2p$ and $3p$ levels. The values in the parentheses give the estimates for an excited atom with a $2p$ hole.

Atom	$\Delta_{so}=\frac{3}{2}\lambda$		$\Delta_{ex}=\xi$	
	$2p$	$3p$	$2p$	$3p$
Fe	12.45 (12.95)	1.49 (1.61)	0.84 (0.77)	2.16 (1.64)
Co	14.79 (15.34)	1.81 (1.94)	0.64 (0.34)	1.55 (0.70)
Ni	17.44 (18.08)	2.17 (2.32)	0.26 (0.02)	0.60 (0.04)

11spread in the individual values of λ and ξ given in those papers). Taking into account these observations, we have reduced the calculated values of ξ_{3p} for all considered cases by a factor of 0.5 and have used these scaled values in the MCD calculations.

The mixing coefficients $c_{\nu\mu}^{(\pm)}$ were estimated by solving the eigenvalue problem for the interaction Hamiltonian $H_{\rm int}$ in Eq. (17). In order to appreciate the effect of the exchange interaction on the wave functions $|jl\mu\rangle$ we list here the values of the mixing coefficients for the Fe $2p_{3/2}$ level,

$$c_{3/2,-1/2}^{(+)}=0.99962, \quad c_{3/2,-1/2}^{(-)}=0.02746,$$

$$c_{3/2,1/2}^{(+)}=0.99959, \quad c_{3/2,1/2}^{(-)}=0.02856,$$

and for the Fe $3p_{3/2}$ level,

$$c_{3/2,-1/2}^{(+)}=0.98107, \quad c_{3/2,-1/2}^{(-)}=0.19365,$$

$$c_{3/2,1/2}^{(+)}=0.96577, \quad c_{3/2,1/2}^{(-)}=0.25939.$$

As expected, the influence of the VB spin field is much stronger for the $3p$ level than for the $2p$. Note that the mixing coefficients are different for $+\mu$ and $-\mu$.

The selection rules for the $L_3M_{2,3}M_{2,3}$ Auger transition allow outgoing electron waves of p and f symmetry. Calculation of the partial Auger intensities shows that the outgoing p wave is the dominant decay channel. Only for the final-state component $^1D_2$ the f wave contributes up to 10% of the intensity.

Adherent to the experimental geometry for the measurements described in Sec. II, the calculations were performed with the incidence photon direction perpendicular to the surface and an emission angle of 60° from the surface normal. For comparison with the experimental data, the calculated intensity of each multiplet component was broadened using a Doniach-Sunjic profile[36] with an asymmetry parameter of 0.3 and lifetime parameter equal to 1.5 and 2.5 eV for the triplet and singlet final states, respectively (for the LS-term dependence of the lifetime, see, e.g., Ref. 54). An integral background was introduced in the calculated spectra in order to reproduce the background intensity observed in the experiment.

Note that in the following discussion we will use the LS notation for the multiplet components of the Auger spectra, although they represent mixed states. This is justified because for each multiplet component the admixture of the other components amounts only to a few percent.

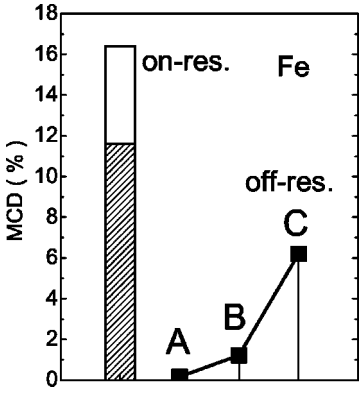

FIG. 2. Comparison of the different contributions to the calculated MCD of the ^3P component in the Fe $L_3M_{2,3}M_{2,3}$ spectra. On-resonance case: MCD obtained without exchange interaction is shown by shaded area. Off-resonance case: A=spin-dependent radial ME, $B=A+$exchange mixing in the $2p$ level, and $C=B+$exchange mixing in the $3p$ level.

V. RESULTS AND DISCUSSION

First, we illustrate in our calculations the role of the various contributions to the MCD signal, where we take the Fe as an example. As discussed in Sec. III, without the influence of the polarized VB states there is no MCD in perpendicular geometry for off-resonance excitation. In this case, the $2p_{3/2}$ intermediate state has no spin polarization.

If we take into account that excited electrons with majority and minority spins are moving in different potentials and, therefore, include the spin dependence of the radial ME's in the calculations, we obtain a tiny MCD signal (Fig. 2, case A). In this case the spin polarization of the $2p_{3/2}$ hole is equal to $P_h=-0.3\%$. If the exchange interaction for the $2p$ shell is switched on (case B), the MCD signal increases to 1%, which is still quite small. The spin polarization of the $2p_{3/2}$ hole is now about -3%, which is the value defined by the exchange interaction for the $2p_{3/2}$ level. In case C the calculation includes the exchange interaction of the core states with the VB electrons for both $2p$ and $3p$ shells. It can be seen from Fig. 2 that just this modification of the wave functions of the $3p$ states determines the final value of MCD.

The on-resonance excitation gives a strong MCD signal which is mainly due to the strong spin polarization of the $2p_{3/2}$ hole. The photoelectron is excited into spin-polarized unoccupied $3d$ states, which results in $P_h=-24.3\%$. If we neglect the exchange interaction and make ξ_{2p} and ξ_{3p} both equal to zero, the spin polarization of the core hole reduces to $P_h=-21.7\%$ and the MCD signal remains still strong (i.e., reduced to $\sim 70\%$; see Fig. 2).

Let us now consider the calculated $L_3M_{2,3}M_{2,3}$ spectra in comparison with the experimental data. As seen from Figs. 3 and 4, the shape of the Auger spectra is mainly determined by the ^1D and ^3P states. The ^1S state has relatively a low intensity, resulting only in a small shoulder. The triplet and singlet states give MCD signals of opposite signs. The MCD spectrum has a positive ^3P-derived peak at the high-energy side and an extended negative structure at the low-energy

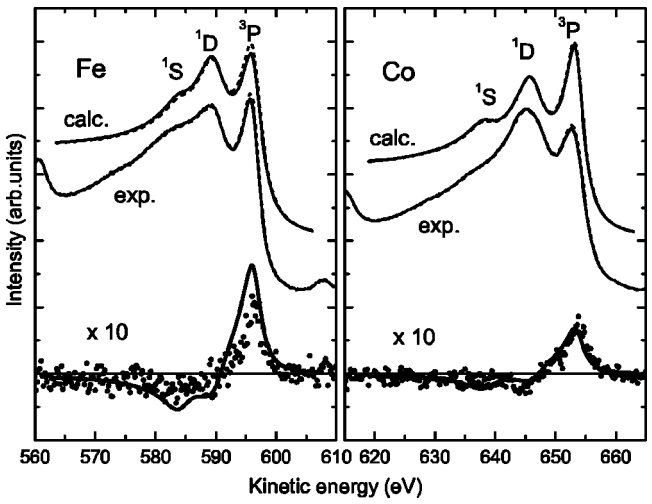

FIG. 3. Off-resonance Fe and Co $L_3M_{2,3}M_{2,3}$ spectra for both helicities and resulting MCD: calculated (solid line) and experimental (dots) results (both $\times 10$).

side with the separate features due to ^1D and ^1S clearly distinguishable.

The individual J contributions in the ^3P state are not resolved in the experiment. The calculations show, however, that the $^3P_0$, $^3P_1$, and $^3P_2$ states have quite different behavior upon a change in the exchange interaction. The most sensitive is the $^3P_1$ state with a drastic increase in the MCD signal if the exchange interaction is included. This increase occurs to a large extent at the cost of the $^3P_2$ state which even reveals a negative intensity difference (with an absolute value of almost half of that of the$^3P_1$) for off-resonance excitation. The $^3P_0$ state shows a weak positive MCD signal. On the other hand, the$^3P_1$ state is not sensitive to the spin polarization caused by the on-resonance excitation. When the exchange interaction is neglected, the $^3P_1$ state shows practically no MCD whereas the $^3P_2$ state shows a strong positive MCD signal and the$^3P_0$ state shows a negative MCD. If the exchange interaction is included, both the $^3P_1$ and $^3P_2$ states contribute to the positive MCD, but the $^3P_0$ state has still a small negative intensity difference.

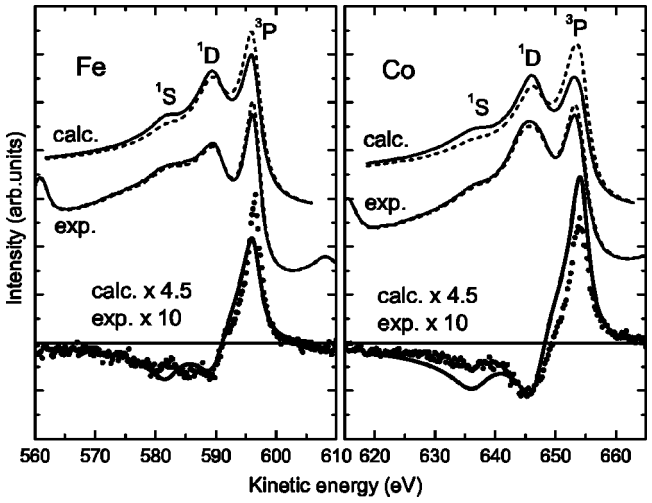

FIG. 4. On-resonance Fe and Co $L_3M_{2,3}M_{2,3}$ spectra for both helicities and resulting MCD: calculated ($\times 4.5$) (solid lines) and experimental ($\times 10$) (dots) results.

For off-resonance excitation (Fig. 3) the calculated and measured results are in very good agreement. In the Fe Auger spectra a strong MCD is observed whereas in the Co spectra the MCD signal is significantly reduced due to the reduced local magnetic moment. As mentioned above, the local magnetic moment in the excited Ni atom practically disappears and no MCD signal is detected experimentally.

For on-resonance excitation (Fig. 4) the calculated MCD signal in Co is stronger than in Fe, which is due to the strong polarization of the unoccupied $3d$ states above the Fermi level that leads to a spin polarization of the $2p$ core hole equal to -44.9% (compared to $P_h=-24.3\%$ in Fe). The MCD signals measured in Fe and in Co are very close to each other. However, the calculated results overestimate the MCD signal and in order to achieve an agreement with the experimental data the calculated intensity has to be scaled down by a factor of 2.22. It should be noted that also the MCD calculations[26] performed for Ni metal using the configuration-interaction method overestimated the experimental MCD signal by a factor of 2.7. More fundamental is probably the fact that also the sum rules[22,23,27] give an MCD signal that is too large by a similar factor. This, however, means that the results of all calculations agree well with those obtained by the sum rules.

Because the theoretical model reproduces the MCD for off-resonance excitation, it seems probable that only the interactions characteristic for on-resonance excitation are responsible for the discrepancy between the calculated and experimental results. The overestimated on-resonance MCD signal is related to an overestimation of P_h in the calculations. This means that either the theoretical description of the polarized photoelectron final states (unoccupied $3d$ states) is not accurate enough or there are relaxation processes that suppress the core-hole polarization in the intermediate state. The calculated results for Fe can be brought in agreement with experiment by narrowing the energy region at E_F that is accessible for threshold photoexcitation, but for Ni the same ''correction'' would increase the discrepancy with the experimental data. In our opinion, the effect of relaxation processes in the intermediate state is more likely. However, this question remains open and requires further consideration.

Additional verification of the theoretical model could come from spin-resolved photoemission measurements. Our calculations predict a difference in the spin polarization of the Auger spectra for different helicities of the incident photons. For example, for off-resonance excitation in Fe the spin polarization is -7.2% (-10.7%) for the ^3P and $+10.7\%$ (-0.7%) for the ^1D with right- (left-) circularly polarized light. A very high spin polarization is inherent for the ^1S state—i.e., $+58\%$ ($+34\%$). However, due to the low intensity and a higher background, this cannot easily be detected experimentally with sufficient accuracy.

In this work we will not compare the shape of the MCD for Ni with the experiment because of the strong correlation effects and resulting satellite structure that have not been taken into account in our theoretical model. In this respect

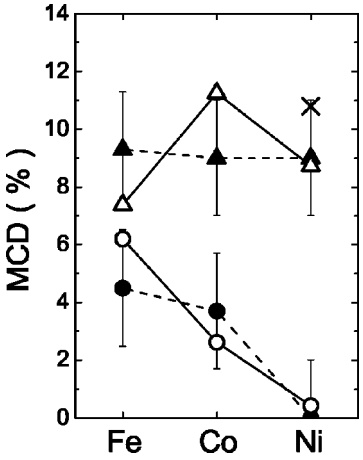

FIG. 5. Comparison of calculated (open symbols) and experimental (solid symbols) MCD (%) of the ^3P component in the Auger $L_3M_{2,3}M_{2,3}$ spectra of the magnetic $3d$ transition metals for on-resonance (triangles) and off-resonance (circles) excitation. The cross indicates the calculated result from Ref. 26. All calculated on-resonance results have been reduced by a factor of 2.22.

we refer to the calculations that include the configuration interaction.[26] Nevertheless, we have estimated for Ni the MCD intensity at the ^3P. All calculated MCD values for Fe, Co, and Ni are collected in Fig. 5 and compared with the experimental data. For off-resonance excitation a strong MCD signal is observed in Fe that decreases going to Co, while in Ni the MCD signal is so tiny that it was not observable experimentally. In the on-resonance Auger spectra the MCD signal is quite strong ($\sim 9\%$) for all $3d$ transition metals considered in the present work.

VI. CONCLUSIONS

We have studied the MCD in the $L_3M_{2,3}M_{2,3}$ Auger spectra of Fe, Co, and Ni for on-resonance (i.e., at the L_3 absorption threshold) and off-resonance excitation (i.e., with primary excitation to a continuum state). The theoretical model takes into account the spin-dependent Auger transition matrix elements for excitation with circularly polarized photons and the partial electron-state configuration in the valence band. In order to describe the MCD effects, the Coulomb interaction between the two holes in the core shell, the core-hole spin-orbit interaction, and the exchange interaction of core states with the spin-polarized VB have been considered on equal footing.

It was shown that the spin field (exchange interaction) acting on the core levels due to the spin-polarized VB is the most important factor for the presence of the observed MCD signal. The singlet (^1S and ^1D) and triplet (^3P) two-hole final states display MCD signals with opposite signs. The prominent peak in the MCD spectrum related to the triplet ^3P final states is the most suitable feature for a quantitative analysis of this signal.

It follows from the theoretical considerations for the Auger-electron emission in perpendicular geometry (i.e., incident photon direction perpendicular to the magnetization direction) that without an exchange interaction there is no MCD observed in the spin-integrated emission for off-resonance excitation. However, an MCD signal can be detected in the spin-resolved Auger-electron spectra or for on-resonance excitation even for negligible exchange interaction. The MCD is strictly symmetry forbidden for Auger emission directions perpendicular to the magnetization vector.

The calculated MCD in the Auger-electron spectra is in good quantitative agreement with the experiment for off-resonance excitation. However, for on-resonance excitation the calculated MCD values overestimate the experimental ones by a factor of 2.2–2.5, in agreement with the reported calculations for Ni metal as well as with the sum rules.

The theoretical model used in the present work does not include certain effects that could modify the energy distribution of the Auger electrons and affect the MCD signal. They are (i) magnetic scattering of the emitted electrons, due to different scattering phase shifts for electrons with majority and minority spins; (ii) surface effects, where the local electronic structure as well as the magnetic moments of the atoms in the surface layer are different from those in the bulk; (iii) different symmetries for the occupied and unoccupied $3d$ valence states (e.g., orbital moment) that can play a role in the orientation dependence of the observed MCD; (iv) Coster-Kronig transitions, such as the $L_2L_3M_{4,5}$, that can change the intermediate $2p_{1/2}$ core hole state into $2p_{3/2}$. Furthermore, a thorough study of the relaxation effects in the intermediate state of the system is required.

Going from Fe to Ni, the MCD displays quite a different behavior for on- and off-resonance excitation. In the off-resonance case the MCD signal decreases due to the reduced local magnetic moment, while for Ni it has practically disappeared. In the on-resonance case the calculations predict the variations of the MCD according to the spin polarization of the unoccupied $3d$ states at the Fermi level; however, these variations are not observed experimentally. The obtained on-resonance MCD signals are very close in Fe, Co, and Ni; the differences between them are within the accuracy of the measurement.

As mentioned, the ratio of the exchange to spin-orbit splitting for the $3p$ level is an important parameter in the theoretical model. However, there is little, if any, consensus on the values of these two quantities (see, e.g., Ref. 44). The sensitivity of the MCD in Auger spectroscopy to the magnitude of the exchange interaction in combination with accurate experimental measurements could in principle be very useful to estimate the parameters of the electron-electron and spin-spin interactions in ferromagnetic solids.

ACKNOWLEDGMENTS

This work was supported by the Deutsche Forschungsgemeinschaft (DFG) under Grant No. 436 UKR 17/14/02. The authors are very grateful to P. Rennert for stimulating discussions and valuable remarks. We acknowledge the European Synchrotron Radiation Facility for beam time, and we are grateful to K. Larsson and N. B. Brookes for the support on beamline ID12B.

[1] *Spin-Orbit-Influenced Spectroscopies of Magnetic Solids*, edited by H. Ebert and G. Schütz (Springer, Berlin, 1996).
[2] G. Schütz, W. Wagner, W. Wilhelm, P. Kienle, R. Zeller, R. Frahm, and G. Materlik, Phys. Rev. Lett. **58**, 737 (1987).
[3] B.T. Thole, P. Carra, F. Sette, and G. van der Laan, Phys. Rev. Lett. **68**, 1943 (1992).
[4] J. Okamoto, H. Miyauchi, T. Sekine, T. Shidara, T. Koide, K. Amemiya, A. Fujimori, T. Saitoh, A. Tanaka, Y. Takeda, and M. Takano, Phys. Rev. B **62**, 4455 (2000).
[5] S. Cherifi, C. Boeglin, S. Stanescu, J.P. Deville, C. Mocuta, H. Magnan, P. LeFèvre, P. Ohresser, and N.B. Brookes, Phys. Rev. B **64**, 184405 (2001).
[6] P. Gambardella, S.S. Dhesi, S. Gardonio, C. Grazioli, P. Ohresser, and C. Carbone, Phys. Rev. Lett. **88**, 047202 (2002).
[7] A. Scherz, H. Wende, K. Baberschke, J. Minár, D. Benea, and H. Ebert, Phys. Rev. B **66**, 184401 (2002).
[8] H.A. Dürr, G.Y. Guo, G. van der Laan, J. Lee, G. Lauhoff, and J.A.C. Bland, Science **277**, 213 (1997).
[9] L. Baumgarten, C.M. Schneider, H. Petersen, F. Schäfers, and J. Kirschner, Phys. Rev. Lett. **65**, 492 (1990).
[10] G. van der Laan, M.A. Hoyland, M. Surman, C.F.J. Flipse, and B.T. Thole, Phys. Rev. Lett. **69**, 3827 (1992).
[11] F.U. Hillebrecht, Ch. Roth, H.B. Rose, M. Finazzi, and L. Braicovich, Phys. Rev. B **51**, 9333 (1995).
[12] X. Gao, M. Salvietti, W. Kuch, C.M. Schneider, and J. Kirschner, Phys. Rev. B **58**, 15 426 (1998).
[13] J. Bansmann, L. Lu, K.H. Meiwes-Broer, T. Schlathölter, and J. Braun, Phys. Rev. B **60**, 13 860 (1999).
[14] F.U. Hillebrecht, H.B. Rose, T. Kinoshita, Yu. Idzerda, G. van der Laan, R. Denecke, and L. Ley, Phys. Rev. Lett. **75**, 2883 (1995).
[15] G.Y. Guo, H. Ebert, W.M. Temmerman, and P.J. Durham, Phys. Rev. B **50**, 3861 (1994).
[16] J. Henk, A.M.N. Niklasson, and B. Johansson, Phys. Rev. B **59**, 13 986 (1999).
[17] B.T. Thole and G. van der Laan, Phys. Rev. B **44**, 12 424 (1991); **48**, 210 (1993); **49**, 9613 (1994).
[18] G. van der Laan, Phys. Rev. B **51**, 240 (1995).
[19] J.G. Menchero, Phys. Rev. B **57**, 993 (1998).
[20] L.H. Tjeng, C.T. Chen, P. Rudolf, G. Meigs, G. van der Laan, and B.T. Thole, Phys. Rev. B **48**, 13 378 (1993).
[21] G. van der Laan, E. Arenholz, Z. Hu, A. Bauer, E. Weschke, Ch. Schüssler-Langeheine, E. Navas, A. Mühlig, G. Kaindl, J.B. Goedkoop, and N.B. Brookes, Phys. Rev. B **59**, 8835 (1999).
[22] B.T. Thole, H.A. Dürr, and G. van der Laan, Phys. Rev. Lett. **74**, 2371 (1995).
[23] G. van der Laan, H.A. Dürr, and M. Surman, J. Electron Spectrosc. Relat. Phenom. **78**, 213 (1996).
[24] H.A. Dürr, G. van der Laan, D. Spanke, F.U. Hillebrecht, and N.B. Brookes, J. Electron Spectrosc. Relat. Phenom. **93**, 233 (1998).
[25] H.A. Dürr, G. van der Laan, and M. Surman, J. Phys.: Condens. Matter **8**, L 7 (1996).
[26] M. Taguchi and G. van der Laan, Phys. Rev. B **66**, 140401 (2002).
[27] G. van der Laan and B.T. Thole, J. Phys.: Condens. Matter **7**, 9947 (1995).
[28] Yu. Kucherenko and P. Rennert, J. Phys.: Condens. Matter **9**, 5003 (1997).
[29] Yu. Kucherenko and P. Rennert, Phys. Rev. B **58**, 4173 (1998).
[30] Yu. Kucherenko, B. Sinković, E. Shekel, P. Rennert, and S. Hulbert, Phys. Rev. B **62**, 5733 (2000).
[31] H.A. Dürr, G. van der Laan, D. Spanke, F.U. Hillebrecht, and N.B. Brookes, Phys. Rev. B **56**, 8156 (1997).
[32] S.S. Dhesi, E. Dudzik, H.A. Dürr, G. van der Laan, and N.B. Brookes, J. Appl. Phys. **87**, 5466 (2000).
[33] O. Gunnarsson and K. Schönhammer, Phys. Rev. B **22**, 3710 (1980).
[34] C.O. Almbladh and L. Hedin, in *Handbook on Synchrotron Radiation*, edited by E.E. Koch (North-Holland, Amsterdam, 1983), Vol. 1, p. 607.
[35] J. Zaanen and G.A. Sawatzky, Phys. Rev. B **33**, 8074 (1986).
[36] S. Doniach and M. Sunjic, J. Phys. C **3**, 285 (1970).
[37] J.B. Pendry, *Low-Energy Electron Diffraction* (Academic Press, London, 1974).
[38] C.S. Fadley, Prog. Surf. Sci. **16**, 275 (1984).
[39] A. Chassé and P. Rennert, Phys. Rev. B **55**, 4120 (1997).
[40] H. Haak, G.A. Sawatzky, and T.D. Thomas, Phys. Rev. Lett. **41**, 1825 (1978).
[41] G.A. Sawatzky, in *Auger Electron Spectroscopy*, edited by C.L. Briant and R.P. Messmer (Academic Press, New York, 1988), p. 168.
[42] D.A. Varshalovich, A.N. Moskalev, and V.K. Khersonskii, *Quantum Theory of Angular Momentum* (World Scientific, Singapore, 1988).
[43] P. Rennert, J. Electron Spectrosc. Relat. Phenom. **119**, 1 (2001).
[44] D.-J. Huang, D.M. Riffe, and J.L. Erskine, Phys. Rev. B **51**, 15 170 (1995).
[45] E.U. Condon and G.H. Shortley, *The Theory of Atomic Spectra* (Cambridge University Press, Cambridge, England, 1991).
[46] I.I. Sobelman, *Atomic Spectra and Radiative Transitions* (Springer, Berlin, 1996).
[47] R.D. Cowan, *The Theory of Atomic Structure and Spectra* (University of California Press, Berkeley, 1981).
[48] P. Rennert, W. Mück, and A. Chassé, Phys. Rev. B **53**, 14 262 (1996).
[49] O.K. Andersen, Phys. Rev. B **12**, 3060 (1975).
[50] H.L. Skriver, *The LMTO-Method* (Springer, Berlin, 1984).
[51] J.P. Perdew and Y. Wang, Phys. Rev. B **45**, 13 244 (1992).
[52] E. Tamura, G.D. Waddill, J.G. Tobin, and P.A. Sterne, Phys. Rev. Lett. **73**, 1533 (1994).
[53] S.H. Baker, K.W. Edmonds, A.M. Keen, S.C. Thornton, C. Norris, and C. Binns, Phys. Rev. B **61**, 5026 (2000).
[54] K. Okada, A. Kotani, H. Ogasawara, Y. Seino, and B.T. Thole, Phys. Rev. B **47**, 6203 (1993).